DINAME 2019 - Proceedings of the XVIII International Symposium on Dynamic Problems of Mechanics,
M.A. Savi, T.G. Ritto and W.M. Bessa (Editors), ABCM, Buzios, RJ, Brazil, March 10th to 15th, 2019

Generalization of the Impedance Matrix Method for Extraordinarily Large-Scale Pile Groups

A. C. A. Vasconcelos and J. Labaki

School of Mechanical Engineering, University of Campinas, SP, Brazil

Abstract: Numerical models of pile groups are a fundamental component of many dynamic soil-structure interaction analyses. Most works consider a small number of piles and soil layers, which is justifiable for ordinary applications. This paper deals with computational issues that arise when extraordinarily large-scale pile groups are considered. A general implementation for dynamic analysis of large-scale pile groups embedded in a viscoelastic layered soil under external loading is presented. Beam equations are used for modeling the piles, whereas Green's functions for layered media are applied to represent the soil. Modern computing tools crafted into the present implementation enable not only massively large pile groups to be modeled, but a nearly arbitrary number of soil layers and excitation frequencies to be considered, which extend the modeling capabilities of the formulation considerably.

Keywords: Large pile groups, parallel computing, dynamic soil-structure interaction

INTRODUCTION

This work is motivated by the construction of Brazil's new synchrotron light source, the Sirius Project (Liu et al., 2014). Particle accelerators such as Sirius typically consist of a large concrete slab supported by an unconventionally large group of piles (Walker, 2003). Figure 1 shows a stage in the construction of the Sirius Project, in which only a small fraction of its foundation can be seen, but which contains a large number of piles. For the Sirius Project, 1330 piles of different geometries were included. Modeling and understanding the dynamic response of such foundations and their energy dissipation and absorption through the soil is fundamental for their remarkably strict vibration requirements to be complied with (Zhao and Xu, 2004).

Figure 1 – Stage of the construction of the Sirius facilities - large group of piles.

The response of pile foundations to external and seismic excitation has been a subject of constant investigation. A considerably general numerical model has been proposed by Kaynia and Kausel (1991), in which piles are represented as elastic beams, the surrounding soil is represented by Green's functions for layered elastic halfspaces, and the coupling between the two systems is obtained by direct equilibrium and kinematic compatibility at the soil-pile interface. Although Kaynia and Kausel's solution provides enough accuracy in modeling the dynamic response of pile groups with regards to their wave propagation response, their implementations are meant for practical application problems in which the number of piles is below a few dozen piles.

This paper presents a generalized, modern implementation of the impedance matrix model of pile groups proposed by Kaynia and Kausel (1991). The present implementation is capable of dealing with as many piles as the physical computing capacity of the computer hardware, which can be easily extended for large CPU and GPGPU clusters. In addition to arbitrary number of piles, the proposed implementation is capable of considering an arbitrary number of soil layers, which enables Gibson's soils and weathered crusts to be modeled (Jin, 2014). An arbitrarily number of excitation frequencies can be considered as well, with which one may obtain accurate impulse responses of the embedded pile group directly through Fourier transforms of the frequency response of the model (Adolph, Mesquita and Romanini, 2003).

FORMULATION

The present generalized implementation is based on a formulation proposed by Kaynia and Kausel (1991). The formulation considers the soil as a layered, transversely isotropic, three-dimensional viscoelastic half-space. Cylindrical horizontal and vertical loads are applied through the depth of each layer, whereas circular loads correspond to pile-tip forces. Generalized expressions for each layer are obtained in terms of arbitrary functions that depend on the boundary conditions of the layers. Upon establishing equilibrium and kinematic compatibility conditions at the layer interfaces, one obtains a system of equation relating interface external forces and displacements for the layered soil system, and these quantities are related through a stiffness matrix of the soil system. Displacements at the center of layers are obtained from the following Hankel transform improper integral

$$I = \int_0^\infty f(k) J_n(kr) J_m(kR) dk, \tag{1}$$

in which $f(k)$ represents a function of Hankel space variable k associated with transformed displacements, J_n and J_m are Bessel functions of n and m order, and r and R are the position and radius of the pile. On the other hand, the piles are modeled as discretized beam bodies consisting of three-dimensional elastic elements under horizontal, axial and bending loads. Each of the pile elements is embedded in each soil layer. The coupling between the pile and its layer is obtained through direct equilibrium and kinematic compatibility at the pile-layer interface. A convenient algebraic matrix equation resulting from the pile-soil layer coupling can be written as

$$\mathbf{P_e} = (\mathbf{K_P} + \Psi^T (\mathbf{F_S} + \mathbf{F_P})^{-1} \Psi) \mathbf{U_e} = \mathbf{K_e} \mathbf{U_e}, \tag{2}$$

where $\mathbf{P_e}$ is the vector of external forces and moments at the two ends of the pile, $\mathbf{K_P}$ is the dynamic stiffness matrix of the pile, Ψ is the dynamic flexibility matrix of clamped-end piles for harmonic end displacements, $\mathbf{F_P}$ and $\mathbf{F_S}$ are, respectively, the flexibility matrix of the pile and the soil, $\mathbf{U_e}$ is the vector of end displacements for pile, and $\mathbf{K_e}$ is the dynamic stiffness for the ensemble of piles. For a detailed description of the quantities involved in Eq. (2), please refer to Kaynia and Kausel (1991).

IMPLEMENTATION

The model proposed by Kaynia and Kausel (1991) is implemented in this work in modern Fortran 90 language, with parallel graphics hardware-enabled routines whenever available (Bourgoin, Chailloux and Lamotte, 2014). The resulting computer code is capable of taking into account as many piles as the physical memory of the computer in which is it executed will allow.

The most demanding computational task in this model is the numerical integration of the Green's functions for the soil part, Eq. (1). The resulting improper integrands are characterized by the presence of singularities and oscillatory-decaying terms, the integral of which only converges at infinity. Extensive work has been done by the authors towards improving the accuracy of that integration, all of which resulted in more computationally expensive integrations (Vasconcelos, Cavalcante and Labaki, 2017; Cavalcante, Vasconcelos and Labaki, 2017; Cavalcante and Labaki, 2018). The most computationally efficient solution for these integrals is through the use of adaptive Gaussian quadratures for both the singular and the oscillatory part of the integrand. A small material damping is included in the constitutive properties of the soil (Christensen, 2012) in order to make the singularities more easily integrable and the oscillatory-decaying tail more quickly decaying. This strategy restricts the application of this implementation to damped media, but this is a reasonable assumption for the present soil problems. Moreover, since each term of the influence matrix $\mathbf{F_S}$ (Eq. (2)) is independent of each other, they can be computed simultaneously. OpenMP routines for parallel CPU execution were incorporated in the implementation for this purpose. The resulting computational cost is only five per cent that of the original serial implementation.

For the solution of the linear system in Eq. (2), a highly optimized numerical package is used (Schenk and Gärtner, 2004), which renders the computer cost of this task insignificant.

NUMERICAL RESULTS

This section brings original numerical results obtained with the present implementation for selected cases. Whenever available, results are compared with Kaynia and Kausel's 1991 original ("reference") implementation.

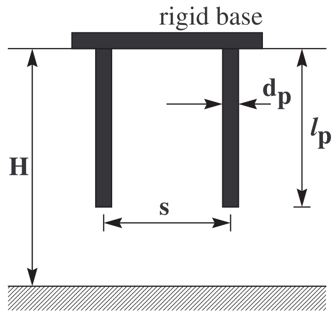

Figure 2 – Validation using a 2×2 pile grid.

Figure 3 shows a comparison of the present with the reference implementation. These results consider the case of a 2x2 group of piles connected by a rigid base (Fig. 2). The pile group is embedded within a homogeneous layer resting on a rigid baserock. The layer has depth $H/d_p = 75$, Poisson's ratio $\nu_s = 0.25$, and material damping ratio $\eta_s = 0.03$, in which d_p is the diameter of the piles and the subindices s and p stand for the soil and the pile, respectively. The piles are characterized by length $L/d_p = 37.5$, Poisson's ratio $\nu_p = 0.25$, and elastic modulus E_p such that $\pi \mu_s L^2/E_p A = 1$, where A is the cross-sectional area of the pile. The results are presented in terms of the dynamic impedance of the pile-soil system, given by

$$K = k + i a_0 c = 1/u \tag{3}$$

where k, c, and u are the stiffness, damping, and displacement of the pile foundation and $a_0 = \omega d_p/c_s$ is the nondimensional frequency of excitation, in which $c_s^2 = \mu_s/\rho_s$ is the largest shear wave velocity of the soil, and $\rho_p/\rho_s = 1$.

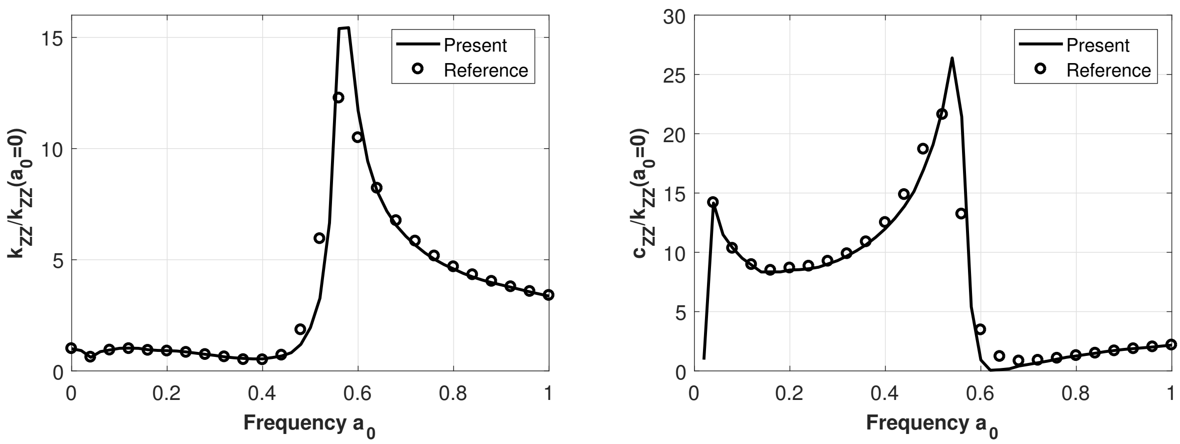

Figure 3 – Vertical stiffness and damping of a 2×2 pile grid connected by a rigid cap.

Figure 3 shows that the present implementation yields accurate numerical results.

Number of piles

The primary goal of the present work is to provide an implementation that is capable of modeling the Sirius Project, with its 1330 piles. The first task was to extend the number of piles N that the computer code is capable of dealing with.

In both the reference and the present implementation, the limiting number of piles is not defined explicitly. Rather, it depends on the arrangement of the piles in the soil. In a square grid of $c \times c$ piles containing $N = c^2$ piles, the reference implementation is limited to 5×5, $N = 25$ piles (Fig. 4).

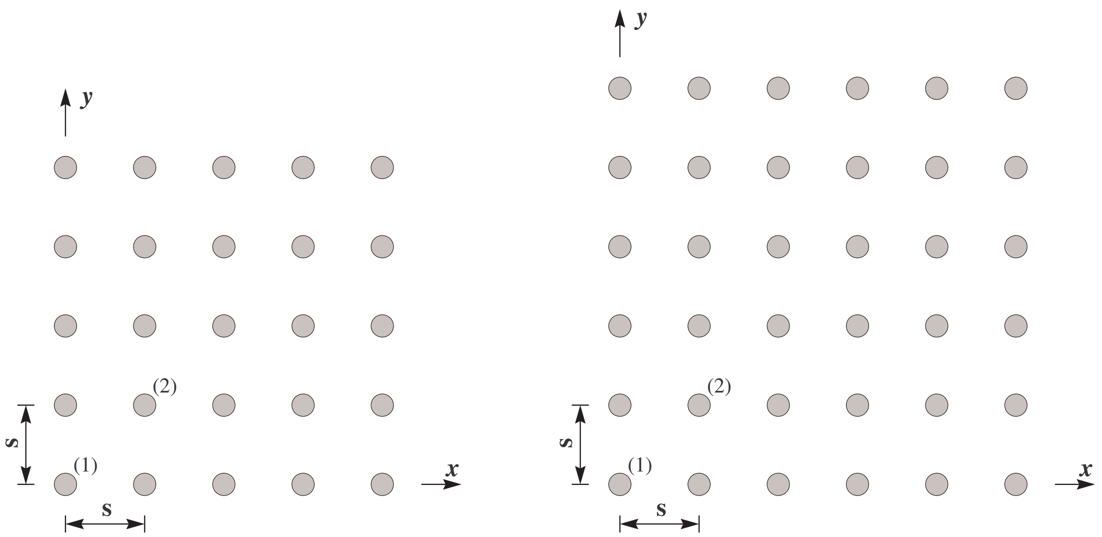

Figure 4 – Pile grids used in this section, with $N = 25$ and $N = 36$ piles.

Figure 5 shows a comparison of this case with the present implementation. These results consider piles of length $l_p/d_p = 1$, $E_p/E_s = 100$, $\rho_p/\rho_s = 2$, $\nu_p = \nu_s$, and pile-to-pile distance $s/d_p = 5$, within a homogeneous, isotropic soil. Pile (1) is under vertical excitation with frequency a_0, and the figures show the resulting normalized vertical displacement $u_z^* = u_z/u_z(a_0 = 0)$ of pile (2). The results show that the present and reference implementations agree for this case.

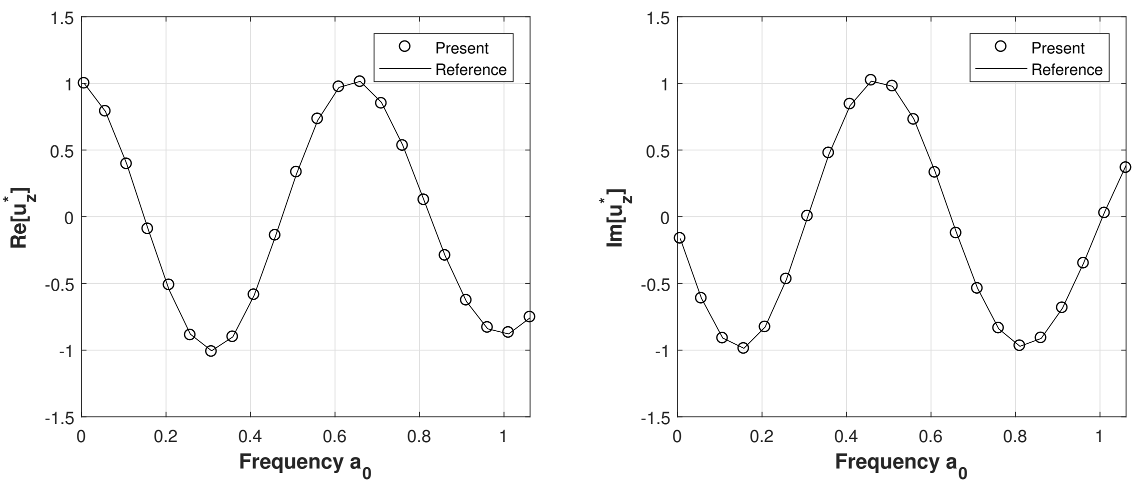

Figure 5 – Vertical displacement of a pile within a 5×5 pile grid.

Figure 6 extends the previous analysis for a 6×6 grid of $N = 36$ piles (Fig. 4b). The reference implementation is unable to model this problem.

The number of piles that the present implementation is capable of considering is limited solely by the physical memory of the hardware in which it is being executed.

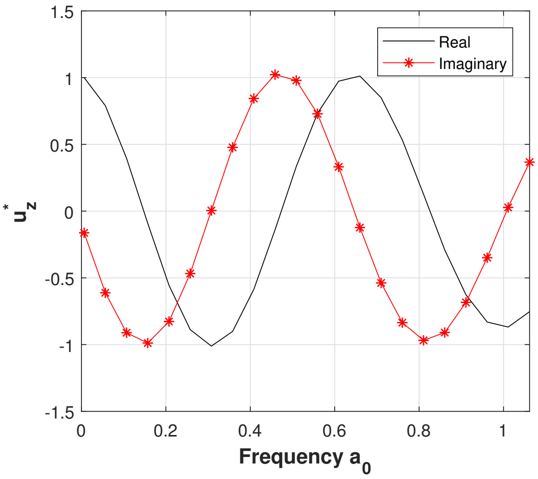

Figure 6 – Vertical displacement of a pile within a 6×6 pile grid.

Number of layers

The reference implementation provides a limit of thirty layers for the soil medium, each of which is associated with one beam element in the pile discretization. This is sufficient to provide good approximations for the traction distribution along the pile for most practical applications (Barros, Labaki and Mesquita, 2018), as well as cases of heterogeneous layered soils with up to thirty different layers. However, a larger number of soil layers would enable the representation of soils with material properties that vary continuously with depth.

Figure 7 illustrates one such case. This is know as Gibson's soil (Jin, 2014), in which the shear modulus μ_s of the soil varies linearly with depth. Figure 7b shows that an insufficient number of layers may not be able to represent the continuous variation of μ_s. It has been shown that an accurate representation of Gibson's soils may require each soil layer to have depth $h_p/d_p \leq 0.25$ (Labaki, Rajapakse and Mesquita, 2018).

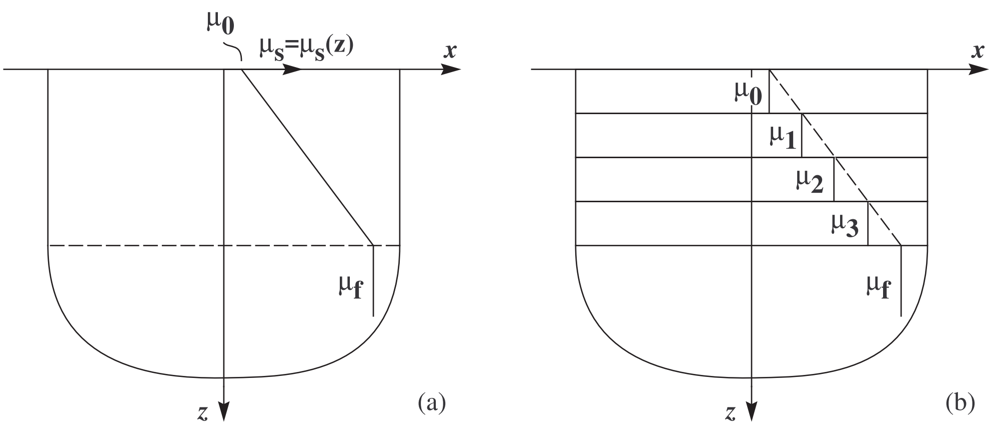

Figure 7 – Soil with continuously varying shear modulus versus discrete heterogeneous layers.

In this section we consider the problem of a pile of length l_p embedded in Gibson's soil with $\mu_s = \mu_0(1 + mz)$. The soil is represented by M homogeneous layers with shear modulus $\mu_i = \mu_0(1 + m \cdot i/Ml_p)$, $i = 1, M$. In this study, $l_p/d_p = 20$, $\mu_p/\mu_0 = 100$, $\rho_p/\rho_s = 2$, $\nu_p = \nu_s$, and $m = 2$.

Figure 8 compares the normalized displacement $u_z^* = u_z/u_z(M = 10)$ of the head of the pile for different numbers of layers and $a_0 = 0.5$. The results show that the response tends monotonically to the value that corresponds to the perfectly continuous variation of shear modulus of the soil. Note that the reference implementation can only go as far as thirty layers. In the present case this does not represent a Gibson's soil model. This conclusion may differ for different values of l_p and m.

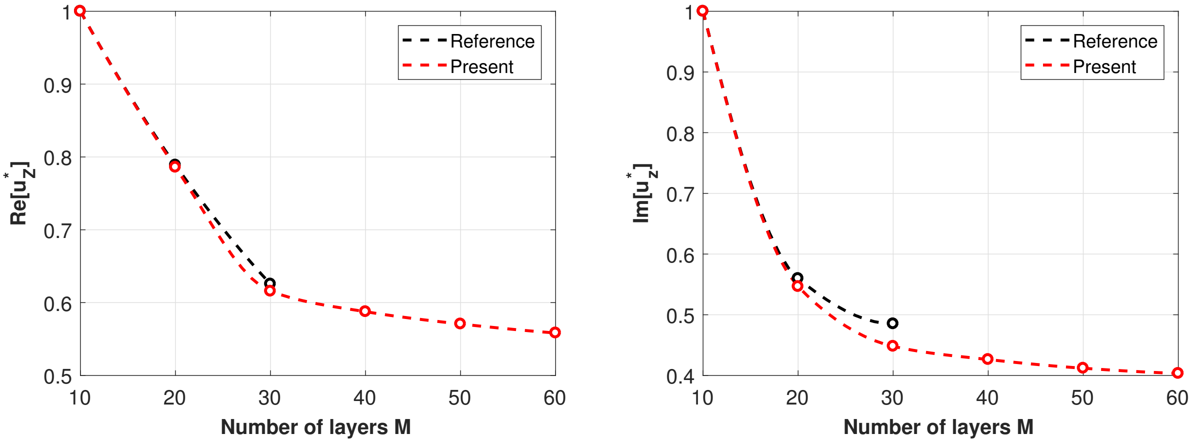

Figure 8 – Convergence of pile response with numbers of layers.

The present implementation can be used to model weathered crusts as well, in which the shear modulus of the soil first decreases up to a certain shallow depth, after which it increases, as well as any other soil model in which shear modulus and mass density vary with depth.

Reach in frequency

In dynamic soil-foundation interaction problems, the frequency of excitation is typically very low - within the seismic range ($a_0 \leq 1$). However, if an implementation is robust enough to yield the response of the system for high frequencies, one can obtain the transient impulse response of such system through an FFT scheme (Adolph, Mesquita and Romanini, 2003).

Figure 9 shows the transient vertical displacement and velocity of the tip of a pile under a vertical impulse load applied at the pile head. Pressure (P) and shear (S) wave fronts travel through the pile from the pile head and reach the pile tip at times $t_i = l_p/c_i$, $i = P, S$, in which $c_P^2 = (\lambda_p + 2\mu_p)/\rho_p$ and $c_S^2 = \mu_p/\rho_p$, λ_p is the Lamé constant of the pile. In the present case, $l_p/d_p = 20$. Figure 9 shows dashed red lines where the pressure and shear waves are expected to arrive at the pile tip. The results show accurate predictions.

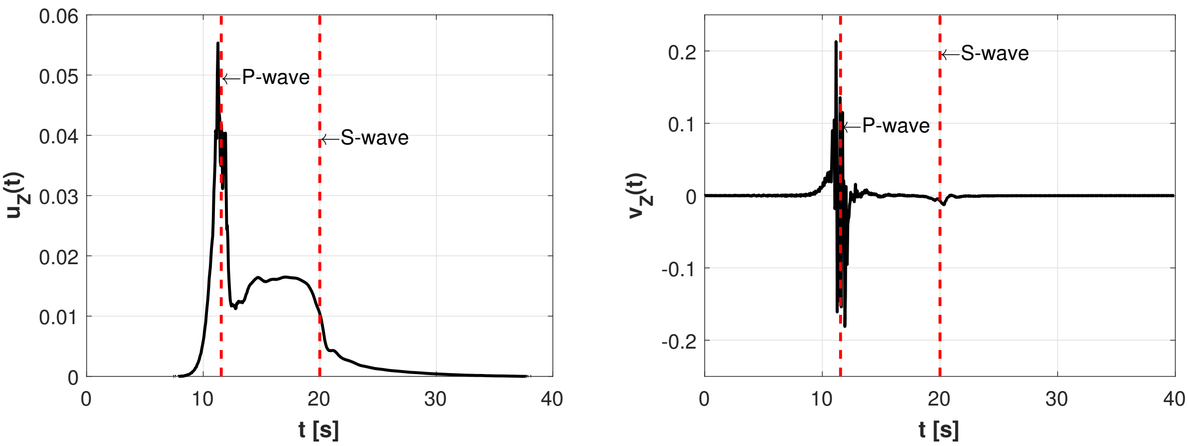

Figure 9 – Impulse response of pile tip.

The transient response of pile groups not only enables additional information about the system, such as a visualization of wavefronts, but can be used together with convolution schemes to yield the response of the system to any other type of excitation (Labaki, Damasceno and Mesquita, 2003).

The discretization in the time domain of the impulse response is directly proportional to the number of values of frequency for which the original time-harmonic signal is computed. The reference implementation is limited to one hundred frequencies. The present implementation is not limited in the number of frequencies it can compute. However, this is merely a convenience feature, since the reference implementation could be executed multiple times if more than one hundred frequencies are necessary. A more substantial improvement in this regard is with respect to the quality of the numerical integration of the influence terms in $\mathbf{F_S}$ (Eq. (2)). The focus of the current stage of the project is in the efficiency of the code, but modern integration schemes that are being implemented into it are already producing more accurate integrations.

Bonding condition

Foundation problems may assume two different bonding conditions at the foundation-soil interface: one in which kinematic compatibility and equilibrium at that interface is enforced in the direction of the loading only, and one in which that is enforced in all directions. The difference between the two bonding conditions is negligible for the problem of surface plates (Labaki, Mesquita and Rajapakse, 2014; Labaki, Rajapakse and Mesquita, 2018) and single piles (Barros, 2006; Barros, Labaki and Mesquita, 2018). The present implementation enables both bonding conditions to be considered.

Figure 10 show the vertical displacements of groups of one, two, and four piles under vertical excitation. Markers and lines show respectively relaxed and fully-bonded contact conditions. Continuous and dashed lines correspond to real and imaginary parts. Figure 11 shows the horizontal displacement of a pile under vertical excitation of frequency $a_0 = 1$. Figures 11a, b, and c show this quantity for three different values of E_p, ρ_p, and l_p, respectively. Each curve within each figure corresponds to a different value of these pile parameters. The parameters used in these analyses are irrelevant in the present paper, as they aim simply to show that the relaxed and fully-bonded contact conditions are indistinguishable for pile groups as well, regardless of the number of piles in the group or their constitutive parameters. For a full description of these cases and a complete analysis of bonding conditions, please refer to Vasconcelos and Labaki (2019).

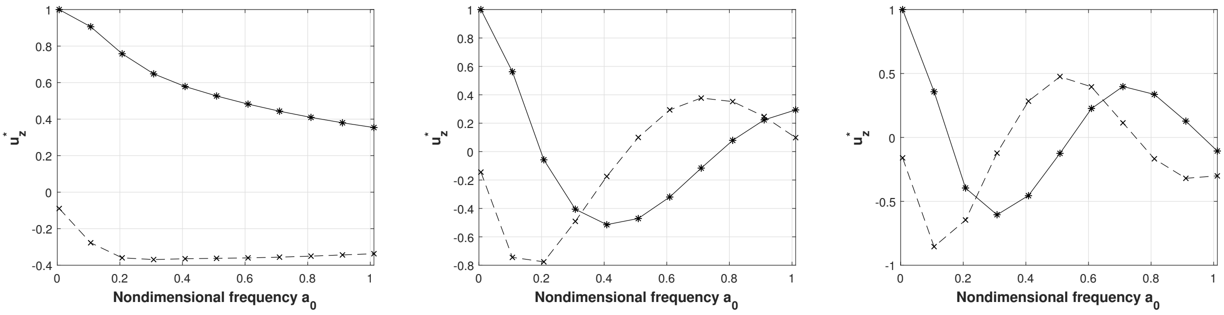

Figure 10 – Real and imaginary part of u_z^* for single, two, and four piles.

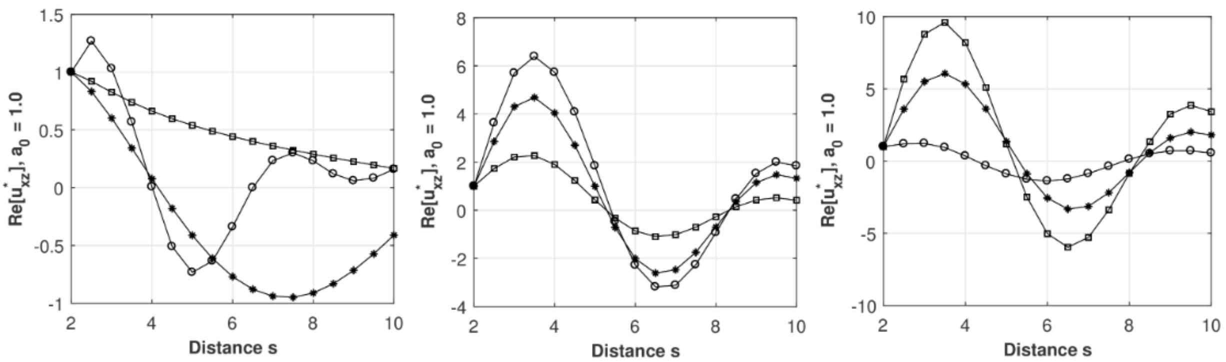

Figure 11 – Normalized cross displacement u_x^* due to a vertical load for one pile and different parameters.

From the computing efficiency point of view, however, the relaxed bonding condition has shown to be from sixteen to eighteen per cent less computationally expensive than the fully-bonded condition.

Numerical precision

The present implementation uses double precision in all of its computations. This is an improvement over the reference implementation's single precision computations. Tables 1 and 2 show an example of results obtained with the two implementations. These are the vertical displacement of pile head and tip for the Gibson's soil problem considered in Fig. 8. Double-precision computing is particularly important for highly detailed analyses such as that in Fig. 9.

Table 1 – Non-normalized vertical displacement of the pile head in single and double precision

M	$u_z^{ref}(z=0)$	$u_z^{present}(z=0)$
10	2.51E-02 - 2.68E-03i	2.533091964329770E-002 - 2.708101515209209E-003i
20	1.98E-02 - 1.50E-03i	1.990730241373737E-002 - 1.479873021093602E-003i
30	1.57E-02 - 1.30E-03i	1.559579569852306E-002 -1.213291072226059E-003i

Table 2 – Non-normalized vertical displacement of the pile tip in single and double precision

M	$u_z^{ref}(z=l_p)$	$u_z^{present}(z=l_p)$
10	-1.27E-04 - 3.94E-05i	-1.185645004647512E-004 - 4.581495383222291E-005i
20	-9.82E-05 - 8.56E-05i	-1.072022351902839E-004 - 8.123614967273680E-005i
30	- 9.45E-05 - 9.86E-05i	-1.018054846131397E-004 - 8.813936429117812E-005i

Computational cost

The number of integrals of Eq. (1) to be evaluated in a given execution of the present code varies quadratically with the number of elements M used in the pile discretization (equal to the number of layers in the system). However, the computational cost due to the integration of Eq. (1) does not vary linearly with $\sqrt{M}$. This is due to the fact that integrals may be more or less difficult to evaluate depending on the parameters of the problem. Table 3 shows the computational cost to solve the case of a single pile discretized by $M = 1, ..., 20$ elements. The table breaks down the total elapsed time Δt into the time spent to fill matrix $\mathbf{F_S}$, $\Delta t_{\mathbf{F}_s}$ (Eq. 2), that is, solve all integrals of Eq. (1) in the formulation, and the time spent to solve the final linear system in Eq. (2), $\Delta t_{Eq.(2)}$. Table 3 shows that the time spent to solve the linear system in Eq. (2) is negligible.

Table 3 – Computational cost of single pile with different numbers of elements M.

M	Δt	$\Delta t_{\mathbf{F}_s}$	$\Delta t_{Eq.(2)}$	M	Δt_{total}	$\Delta t_{\mathbf{F}_s}$	$\Delta t_{Eq.(2)}$
1	1.377	1.277	0.100	11	78.523	78.423	0.100
2	2.677	2.576	0.101	12	100.698	100.589	0.109
3	5.099	4.998	0.101	13	121.613	121.504	0.109
4	7.941	7.841	0.100	14	148.737	148.627	0.110
5	14.183	14.081	0.100	15	169.977	169.852	0.109
6	18.187	18.087	0.100	16	212.661	212.558	0.101
7	26.879	26.778	0.101	17	251.851	251.749	0.101
8	37.606	37.504	0.100	18	307.368	307.265	0.101
9	47.754	47.652	0.100	19	333.696	333.585	0.111
10	61.757	61.648	0.100	20	412.041	411.939	0.100

Additionally, Table 4 shows the time spent to solve the cases of $N = 1, ..., 6$ piles of $M = 20$ elements each.

Figure 12a shows that the cost to solve this problem increases slightly more than linearly with the number of integrals to be solved. Figure 12b shows that the addition of new piles with the same geometry and properties increases the computational cost of the solution in an irregular manner.

An extrapolation of Table 4 yields the daunting conclusion that a case study of Sirius Project's 1330 piles would take thirty-three centuries to finish computing, in the current implementation.

Table 4 – Computational cost of a pile group with N piles.

N	Δt	$\Delta t_{Eq.(2)}$
1	412.041	0.100
2	1185.538	0.109
3	1942.404	0.102
4	2950.984	0.105
5	3045.961	0.140
6	3990.635	0.125

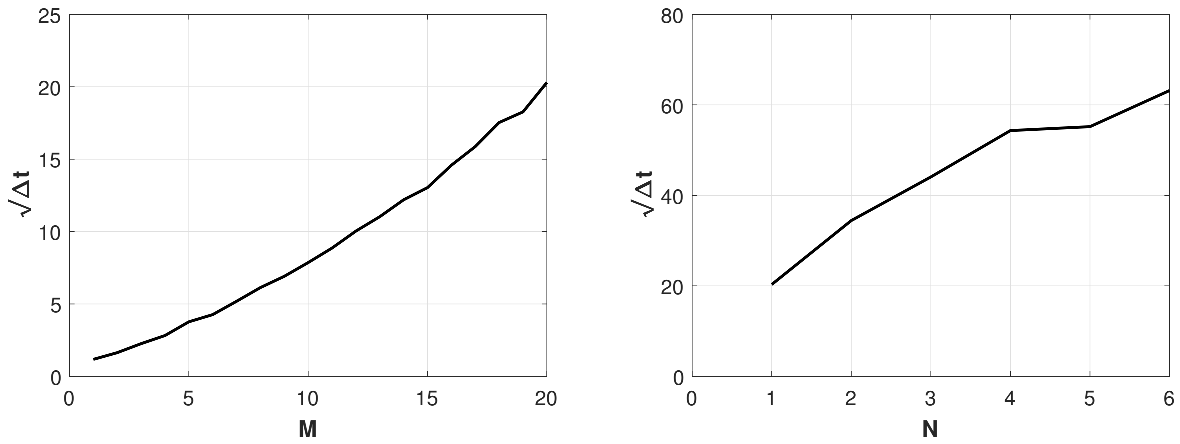

Figure 12 – Total computational cost to solve a single pile with M elements and N piles with $M = 20$ elements.

CONCLUDING REMARKS

The present paper introduced a generalized implementation of the impedance matrix model of pile groups proposed by Kaynia and Kausel (1991) in a modern, parallelizable computer language, with the aim of executing an arbitrarily large group of piles. The implementation is capable of reproducing previous results from the literature, especially from Kaynia and Kausel's previous implementation. The most computationally expensive portions of the code were identified and dealt with appropriately. A reduction of twenty times in the cost of evaluating numerical integrals was obtained by the parallelization of that portion of the code. Another sixteen to eighteen per cent acceleration was obtained by incorporating less expensive pile-soil bonding conditions, without loss of physical consistency. An arbitrarily large number of piles can be considered, within the (extensible) bounds of physical hardware limitations.

ACKNOWLEDGMENTS

The research leading to this article has been funded in part by the Sao Paulo Research Foundation - Fapesp, through grant 2017/01450-0. The support of Capes, CNPq, and Faepex-Unicamp is also gratefully acknowledged.

REFERENCES

Adolph, M., Mesquita, E. and Romanini, 2001, A methodology to determine the transient response of the structures interacting with visco-elastic soils using the FFT algorithm. Proceedings of XXI Iberian-Latin-American Congress on Computational Methods in Engineering, Vol. 1, pp.1-23, Campinas, Brazil.

Barros, P. L. A., 2006, Impedances of rigid cylindrical foundations embedded in transversely isotropic soils. International Journal for Numerical and Analytical Methods in Geomechanics, 30(7):683702.

Barros, P. L. A., Labaki, J. and Mesquita, E., 2018, IBEM-FEM Model of a Piled Plate Within a Transversely Isotropic Half-Space, Engineering Analysis with Boundary Elements (*in press*).

Bourgoin, M., Chailloux, E. and Lamotte, J.L., 2014, Efficient abstractions for GPGPU programming. International Journal of Parallel Programming, Vol. 42, No. 4, pp.583-600.

Cavalcante, I. and Labaki, J., 2018, An Extension of Longman's Method for the Integration of Beating, Oscillatory-Decaying Functions, Proceedings of United States National Congress for Applied and Theoretical Mechanics, Chicago.

Cavalcante, I., Vasconcelos, A. C. A. and Labaki, J., 2017, A Continuation Algorithm-Longman's Method Scheme for the Integration of Transcendental Functions, Proceedings of the Iberian Latin American Congress on Computational Methods in Engineering, Florianopolis.

Christensen, R., 2012. Theory of viscoelasticity: an introduction. Elsevier.

Jin, J.M., 2014, Solutions for Axisymmetric Problems of Layered Generalized Gibson Subgrade. Applied Mechanics and Materials, Vol. 574, pp. 53-57. Trans Tech Publications.

Kaynia, A. M. and Kausel, E., 1991, Dynamics of Pile and Pile Groups in Layered Soil Media, Soil Dynamics and Earthquake Engineering, Vol.10, pp. 386-401.

Labaki, J., Damasceno, D. A. and Mesquita E., 2003, Transient Response of Rigid Foundations Embedded in Transversely Isotropic Media Through an Intertive Dynamic Coupling Scheme. In: International Conference on Computational & Experimental Engineering and Sciences, Seattle.

Labaki, J., Mesquita, E. and Rajapakse, R.K.N.D., 2014. Vertical Vibrations of an Elastic Foundation with Arbitrary Embedment within a Transversely Isotropic, Layered Soil. Computer Modeling in Engineering & Sciences, 103(5), pp.281-313.

Labaki, J. Rajapakse, R. K. N. D. and Mesquita, E., 2018. Dynamic Response of a Rigid Circular Foundation in Layered Anisotropic and Gibsons Soils, Gotechnique (*submitted*).

Liu, L., Milas, N., Mukai, A.H., Resende, X.R. and de S, F.H., 2014, The Sirius Project. Journal of synchrotron radiation, Vol. 21, No.5, pp.904-911.

Schenk, O. and Gärtner, K., 2004. Solving unsymmetric sparse systems of linear equations with PARDISO. Future Generation Computer Systems, 20(3), pp.475-487.

Vasconcelos, A. C. A., Cavalcante, I. and Labaki, J., 2017, On the Accuracy of Adaptive Quadratures in the Numerical Integration of Singular Green's Functions for Layered Media, Proceedings of the Iberian Latin American Congress on Computational Methods in Engineering, Florianopolis.

Vasconcelos, A.C.A. and Labaki, J., 2019, Influence of pile-pile coupling conditions in the vibration of piles groups, Proceedings of of the 7^{th} International Symposium on Solid Mechanics, São Carlos, Brazil.

Walker, R.P., 2003, May. Progress with the Diamond light source project. In PAC (Vol. 3, p. 232).

Zhao, Z.T. and Xu, H.J., 2004. SSRF: A 3.5 GeV synchrotron light source for China. In Proceeding of EPAC (Vol. 2004).

RESPONSIBILITY NOTICE

The authors are the only responsible for the printed material included in this paper.